Online ISSN 1848-3380, Print ISSN 0005-1144
ATKAFF 57(1), 89–98(2016)

Mohammad Mahdi Rezaei, Jafar Soltani

Sliding Mode Control of a Grid-Connected Distributed Generation Unit under Unbalanced Voltage Conditions

DOI 10.7305/automatika.2016.07.870
UDK 681.511.4:621.311.68.072; 517.977.15

Original scientific paper

The increasing presence of inverter-based distributed generation (DG) units in distribution networks (DNs) requires control methods that achieve high performance not only during normal operating conditions, but also under unbalanced conditions. With a high probability, a type of voltage unbalance in DNs is unequal three-phase voltage magnitudes at the fundamental system frequency. This can occur temporarily due to faults or permanently due to uneven distribution of unbalanced loads, on the three-phases of the DN. This paper proposes a sliding mode (SM) based controller for grid-connected DG units, under unbalanced grid voltage condition. The proposed control strategy employs a nonlinear control scheme to directly cancel out the negative-sequence (NS) components of DG output current under unbalanced voltage condition; and directly regulate the positive-sequence (PS) active and reactive power injected by DG units to main-grid. The control method proposed in this paper is shown to be robust and stable system parameter uncertainties. The validity and effectiveness of the proposed controller is verified by using time-domain simulation studies, under the MATLAB/Simulink software environment.

Key words: Distributed generation, voltage source converter, sliding mode control, unbalanced voltage

Upravljanje proizvodnom jedinicom spojenom na mrežu tijekom nesimetričnih napona na mreži temeljeno na kliznom režimu. Povećanje udjela distribuiranih proizvodnih jedinica povezanih na mrežu frekvencijskim pretvaračima zahtjeva metode upravljanja koje dobro djeluju tijekom normalnih uvjeta na mreži kao i u nesimetričnim uvjetima. Najčešći tip nesimetričnog napona na distribuiranoj jedinici je nesimetrična amplituda trofaznog napona na fundamentalnoj frekvenciji. To se događa privremeno zbog kvarova ili trajno zbog nejednake distribucije nesimetričnih tereta na tri faze distribuirane proizvodne jedinice. U ovom radu predlaže se regulator temeljen na kliznom režimu za upravljanje proizvodnom jedinicom spojenom na mrežu tijekom nesimetričnih napona na mreži. Predložena strategija upravljanja koristi nelinearnu shemu upravljanja kako bi se izravno poništile inverzne komponente izlazne struje tijekom nesimetričnih uvjeta; i izravno upravlja direktnom komponentom radne i jalove snage isporučene u mrežu. Metoda upravljanja predložena u ovom radu pokazala se kao robusna i stabilna uz nesigurne parametre sustava. Opravdanost i učinkovitost predloženog regulatora provjerena je korištenjem simulacija u MATLAB/Simulinku.

Ključne riječi: distribuirana proizvodnja, mrežni pretvarač, klizni režim upravljanja, nesimetrični napon

1 INTRODUCTION

Recently, due to a general increasing demand for electrical energy and a rising interest in clean technologies, the energy sector is moving to the era of distributed energy resources (DERs), such as wind turbines, photovoltaic systems, fuel-cells, micro-turbines and hydropower turbines [1-2]. Typical modern distributed generation (DG) units, which are collectively referred to DERs, do not generate 50/60 Hz ac voltages and therefore require electronic power converters as the interfacing medium between a prime energy source and the network [3-4]. These interfaces turn the DG sources more flexible in their control and operation compared to the conventional synchronous machines. In addition, a power electronic converter can mitigate harmonic and unbalanced load or source problems. However, due to their relatively low inertia, these interfaces also turn the system potentially susceptible to the network disturbances [5].

A DG unit can be operated either in grid-connected mode or in islanding mode. Normally, DG units operate in grid-connected mode because the utility grid can support the system frequency and voltage by covering the power mismatch immediately. In the grid-connected operation, the DG unit is connected to the main-grid at the point of common coupling (PCC), and generates proper real and reactive power [6-7]. In this mode, most of the system-level

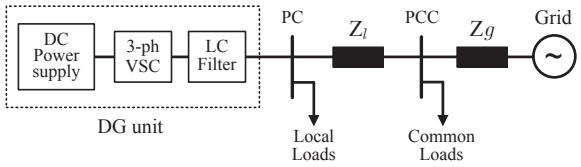

Fig. 1. Schematic diagram of the DG system under consideration

dynamics are dictated by the main-grid due to the relatively small size of DGs. The sensitiveness of DG unit to utility grid disturbances is a major drawback of this mode [8]. In the grid-connected mode, the power inverters forming DG system is continuously exposed to the abnormal conditions and disturbances existing in the grid [9]. The most severe cause of abnormal conditions in the main-grid are short-circuiting faults, unbalanced distribution of single phase loads and starting up of large induction machines, as these are common in distribution levels [10,11]. These events normally produce steady-state and transient voltage unbalances. Operation of DG units under voltage unbalances has not received much attention in the past, since many grid operators demand the immediate disconnection of DG in case of grid disturbances as prerequisite for grid-connection. However, as the power generated by DG units increases, this behavior stresses the main-grid and could cause power unbalance, which may turn into instability. Therefore, the interaction between DG units and main-grid during voltage unbalanced conditions is very important and it must be considered when designing a proper control strategy [12]. In the literature, it can be seen that a part of research effort in the area of DG systems has been dedicated to the grid-connected-mode control of inverter-based DG units under unbalanced voltage conditions [13-17].

Table 1. System parameters

Grid voltage, Line to Line, rms	V_{s-rms}	380 V
Fundamental frequency	f_s	50 Hz
Grid resistance	R_g	0.020 Ω
Grid inductance	L_g	200 μH
Line resistance	R_l	0.050 Ω
Line inductance	L_l	100 μH
DC bus voltage	V_{dc}	800 V
Filter resistance	R_f	0.050 Ω
Filter inductance	L_f	800 μH
Filter capacitance	C_f	200 μF
Switching frequency	f_{sw}	6480 Hz

A vector control approach for controlling the voltage sourced converter (VSC) which is capable of mitigating the harmonics under unbalanced operating conditions is proposed in [13]. Positive- and negative-sequence components of the output current have been controlled independently with a dual control scheme, in which the current references can be accurately selected with the purpose of avoiding second harmonic oscillations in the active power flow of the converter, and by that reducing oscillation in the DC-link voltage. However, a constant DC bus voltage is achieved at the cost of unbalanced grid currents, and these results in a decrease of maximum deliverable power [14,15]. As it can be seen in [13], the presented vector control approach requires two reference frame transformation modules for voltage and current, two real-time sequence extraction algorithms also for voltage and current, and two synchronous current reference generation systems (one for each rotating sequence). Therefore, the presented control scheme is complex [9].

Early publications related to control of VSCs during unbalanced conditions [14-17], have presented generalized discussions on how to derive current references corresponding to different objectives for control of active and reactive powers during unbalanced conditions [15]. The control scheme proposed in [14,15] is based on either grid voltage oriented [14] or grid virtual-flux-oriented [15] vector control. The scheme decouples the DG current into active and reactive power components. Control of instantaneous active and reactive powers is then achieved by regulating the decoupled DG currents, using proportional-integral (PI) or proportional-resonance (PR) controllers. One main drawback for this control scheme is that the performance highly relies on the tuning of the PI or PR parameters and accurate system parameters. Hence, performance may degrade when actual system parameters deviate from values used in the control system [17].

A direct power control (DPC) strategy has been presented in [16,17] for a grid-connected VSC under voltage unbalanced conditions. The DPC scheme is based on the SM control approach, which controls the instantaneous active and reactive powers in the stationary reference frame. Three power control targets have been proposed during network unbalance to obtaining sinusoidal and symmetrical grid current, removing reactive power ripples, and canceling active power ripples. However in the chosen study system, the VSC is directly connected to main-grid and the PCC voltage dynamics are ignored that makes the system control very simple. In addition, the NS power control method has been designed based on knowledge of actual values of the resistances and inductances of the system. Hence, the system stability is not guaranteed with subject to system parametric uncertainties.

The main contribution of this paper is to use the well-known sliding mode control technique in order to improve the performance of the DG control systems when an unbalanced drop in the grid voltage occurs. The proposed control strategy employs a NS current controller, which is designed to compensate the NS component of DG output

currents; and a PS power controller, which is designed to directly regulate the PS active and reactive powers generated by DG units. In order to overcome the computational burden associated with the tracking of grid voltage phase angle and frame transformations, the proposed controllers are performed in stationary reference frame. Time-domain simulation results are presented to demonstrate the validity and effectiveness of the proposed control method.

2 SYSTEM DESCRIPTION AND MODELLING

A single-line diagram of the DG study-system used in this paper is shown in Fig. 1. The DG unit is represented by a DC power supply, a VSC, and a LC-filter that is connected to point of connection (PC). The local loads of the DG unit are connected to the PC and, the common loads are connected to the PCC. The interlink-lines between PC and PCC is represented by a series RL branch. In this paper, it is assumed that the DG system is connected to main-grid. The system parameters are given in Table 1.

Fig. 2 shows the control structure of the inverter-based DG unit. Using well-known Clarke transformation, the current and voltage dynamics in the stationary ($\alpha\beta$) reference frame can be derived as:

$$\frac{\mathrm{d}\mathbf{i}_f}{dt} = -\frac{R_f}{L_f}\mathbf{i}_f + \frac{1}{L_f}\left(\mathbf{v}_i - \mathbf{v}_f\right) \tag{1}$$

$$\frac{\mathrm{d}\mathbf{v}_f}{dt} = \frac{1}{C_f}\left(\mathbf{i}_f - \mathbf{i}_o\right) \tag{2}$$

It is assumed that the LC-filter and the interlink-line have balanced three-phase impedance since, each of the equations (1)-(2) can be fully decoupled into positive and negative sequences. Under unbalanced condition, each of voltages and currents can be expressed as [18]:

$$\mathbf{v} = [v_\alpha\ v_\beta]^T = [(v_\alpha^p + v_\alpha^n)\ (v_\beta^p + v_\beta^n)]^T \tag{3}$$

$$\mathbf{i} = [i_\alpha\ i_\beta]^T = [(i_\alpha^p + i_\alpha^n)\ (i_\beta^p + i_\beta^n)]^T \tag{4}$$

Since the whole controller is designed in the stationary reference frame, the sequence detection of system voltages and currents is also realized based on a stationary frame notch filter in the $\alpha\beta$-frame [19]. It should be note that the case of grid voltage and frequency deviations is out of scope of this paper. However, as stated in [19], the applied method is robust to small-frequency variations so that a high-performance output can be achieved even under a distorted grid voltage [14]. Although according to the allowable limits of frequency-deviation of main-grid [20], a phase-locked loop (PLL) can be avoided in the grid-connected mode [14],[19], for adapting to larger-frequency changes, a PLL or a frequency adaption loop can be added to the applied filter [19],[21].

3 SLIDING MODE CONTROL DESIGN

The proposed control structure consists of a PS power controller and a NS current controller, as shown in Fig. 2. The power controller is designed to regulate the PS active and reactive power injected by DG unit to the system, under both balanced and unbalanced conditions. The NS current controller is designed to compensate the impact of the grid voltage imbalance, on the DG output current. In the subsequent sections, the control design procedure is explained in detail.

3.1 Positive-sequence power control

The instantaneous active and reactive power injected by DG unit to the system can be represented as [15]:

$$P = \frac{3}{2}\left(\mathbf{v}_f \cdot \mathbf{i}_f\right) = \frac{3}{2}\left(v_{f\alpha} i_{f\alpha} + v_{f\beta} i_{f\beta}\right) \tag{5}$$

$$Q = -\frac{3}{2}\left|\,\mathbf{v}_f \times \mathbf{i}_f\right| = \frac{3}{2}\left(v_{f\beta} i_{f\alpha} - v_{f\alpha} i_{f\beta}\right) \tag{6}$$

where "$\cdot$" denotes the inner-product while "$\times$" represents the cross-product of two vectors and bold symbols represent$\mathbf{v}_f = [v_{f\alpha}\ v_{f\beta}]^T$ and $\mathbf{i}_f = [i_{f\alpha}\ i_{f\beta}]^T$. Under unbalanced conditions, the instantaneous active and reactive powers can be expressed by the PS and NS components of the voltages and currents as given by (7) and (8), respectively [15].

$$P = P^p + P^n + P^{2\omega} \tag{7}$$

$$Q = Q^p + Q^n + Q^{2\omega} \tag{8}$$

with

$$\begin{bmatrix} P^p \\ Q^p \end{bmatrix} = \frac{3}{2}\begin{bmatrix} v_{f\alpha}^p & v_{f\beta}^p \\ v_{f\beta}^p & -v_{f\alpha}^p \end{bmatrix}\begin{bmatrix} i_{f\alpha}^p \\ i_{f\beta}^p \end{bmatrix} \tag{9}$$

$$\begin{bmatrix} P^n \\ Q^n \end{bmatrix} = \frac{3}{2}\begin{bmatrix} v_{f\alpha}^n & v_{f\beta}^n \\ v_{f\beta}^n & -v_{f\alpha}^n \end{bmatrix}\begin{bmatrix} i_{f\alpha}^n \\ i_{f\beta}^n \end{bmatrix} \tag{10}$$

$$\begin{bmatrix} P^{2\omega} \\ Q^{2\omega} \end{bmatrix} = \frac{3}{2}\begin{bmatrix} v_{f\alpha}^n & v_{f\beta}^n \\ v_{f\beta}^n & -v_{f\alpha}^n \end{bmatrix}\begin{bmatrix} i_{f\alpha}^p \\ i_{f\beta}^p \end{bmatrix} + \frac{3}{2}\begin{bmatrix} v_{f\alpha}^p & v_{f\beta}^p \\ v_{f\beta}^p & -v_{f\alpha}^p \end{bmatrix}\begin{bmatrix} i_{f\alpha}^n \\ i_{f\beta}^n \end{bmatrix} \tag{11}$$

Noting that under balanced conditions, the NS components of voltages and currents are zero and thus, the instantaneous powers are equal to PS power components. It means that under both balanced and unbalanced conditions, the PS active and reactive powers should be controlled. For this aim, the following integral-based sliding surface is selected.

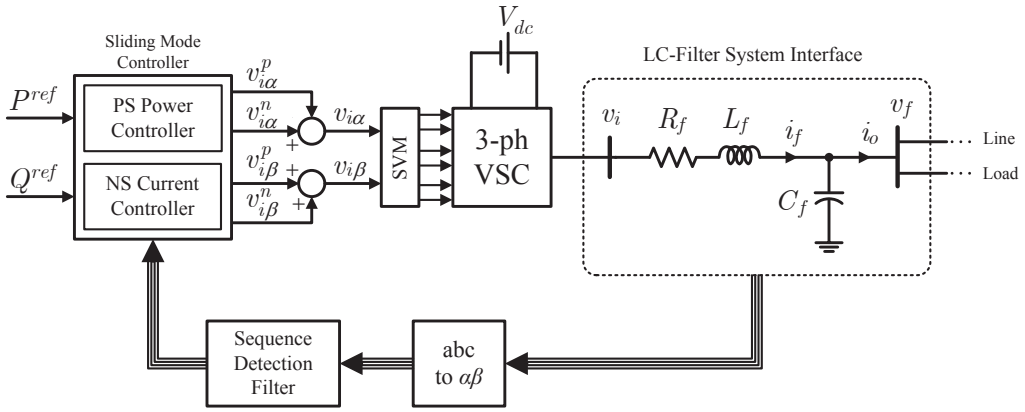

Fig. 2. Proposed control scheme.

$$\begin{bmatrix} S_P \\ S_Q \end{bmatrix} = \begin{bmatrix} e_P \\ e_Q \end{bmatrix} + k_s \int_0^t \begin{bmatrix} e_P \\ e_Q \end{bmatrix} d\tau \qquad (12)$$

where $e_P = P^{ref} - P^p$ and $e_Q = Q^{ref} - Q^p$ are the active and reactive power tracking errors, and $k_s = \mathrm{diag}[k_{sP}, k_{sQ}]$ is a diagonal matrix with all positive constant diagonal entries which are the SM control gains. Based on SM control theory, it is required to restrict the controlled states onto its corresponding sliding surfaces [22]. This is exclusively governed by:

$$S = \frac{dS}{dt} = 0 \qquad (13)$$

Considering (13), differentiating (12) with respect to time gives:

$$\frac{\mathrm{d}}{\mathrm{dt}}\begin{bmatrix} S_P \\ S_Q \end{bmatrix} = \frac{\mathrm{d}}{\mathrm{dt}}\begin{bmatrix} P^{ref} - P^p \\ Q^{ref} - Q^p \end{bmatrix} + k_s \begin{bmatrix} e_P \\ e_Q \end{bmatrix} = -\frac{\mathrm{d}}{\mathrm{dt}}\begin{bmatrix} P^p \\ Q^p \end{bmatrix} + k_s \begin{bmatrix} e_P \\ e_Q \end{bmatrix} \qquad (14)$$

By considering (9), it can be obtained that:

$$\begin{bmatrix} \frac{dP^p}{dt} \\ \frac{dQ^p}{dt} \end{bmatrix} = \frac{3}{2}\begin{bmatrix} \frac{\mathrm{d}v^p_{f\alpha}}{\mathrm{dt}} & \frac{\mathrm{d}v^p_{f\beta}}{\mathrm{dt}} \\ \frac{\mathrm{d}v^p_{f\beta}}{\mathrm{dt}} & -\frac{\mathrm{d}v^p_{f\alpha}}{\mathrm{dt}} \end{bmatrix} \begin{bmatrix} i^p_{f\alpha} \\ i^p_{f\beta} \end{bmatrix} + \frac{3}{2}\begin{bmatrix} v^p_{f\alpha} & v^p_{f\beta} \\ v^p_{f\beta} & -v^p_{f\alpha} \end{bmatrix} \begin{bmatrix} \frac{\mathrm{d}i^p_{f\alpha}}{\mathrm{dt}} \\ \frac{\mathrm{d}i^p_{f\beta}}{\mathrm{dt}} \end{bmatrix} \qquad (15)$$

Substituting for $\frac{\mathrm{d}}{\mathrm{dt}} v^p_{f\alpha\beta}$ and $\frac{\mathrm{d}}{\mathrm{dt}} i^p_{f\alpha\beta}$, respectively from (2) and (1), into (15), results in:

$$\begin{bmatrix} \frac{dP^p}{dt} \\ \frac{dQ^p}{dt} \end{bmatrix} = \frac{3}{2\mathrm{C_f}}\begin{bmatrix} \left(i^p_{f\alpha} - i^p_{o\alpha}\right) & \left(i^p_{f\beta} - i^p_{o\beta}\right) \\ \left(i^p_{f\beta} - i^p_{o\beta}\right) & -\left(i^p_{f\alpha} - i^p_{o\alpha}\right) \end{bmatrix} \begin{bmatrix} i^p_{f\alpha} \\ i^p_{f\beta} \end{bmatrix} + \frac{3}{2\mathrm{L_f}}\begin{bmatrix} v^p_{f\alpha} & v^p_{f\beta} \\ v^p_{f\beta} & -v^p_{f\alpha} \end{bmatrix} \begin{bmatrix} \left(v^p_{i\alpha} - v^p_{f\alpha} - R_f i^p_{f\alpha}\right) \\ \left(v^p_{i\beta} - v^p_{f\beta} - R_f i^p_{f\beta}\right) \end{bmatrix} \qquad (16)$$

By substituting for $\frac{\mathrm{d}}{\mathrm{dt}} P^p$ and $\frac{\mathrm{d}}{\mathrm{dt}} Q^p$ from (16) into (14), it can be shown that:

$$\frac{\mathrm{d}}{\mathrm{dt}}\begin{bmatrix} S_P \\ S_Q \end{bmatrix} = -\begin{bmatrix} G_P \\ G_Q \end{bmatrix} - \begin{bmatrix} H_P \\ H_Q \end{bmatrix} - \frac{3}{2\mathrm{L_f}}\begin{bmatrix} v^p_{f\alpha} & v^p_{f\beta} \\ v^p_{f\beta} & -v^p_{f\alpha} \end{bmatrix}\begin{bmatrix} v^p_{i\alpha} \\ v^p_{i\beta} \end{bmatrix} + k_s \begin{bmatrix} e_P \\ e_Q \end{bmatrix} \qquad (17)$$

with

$$G_P = \frac{3}{2\mathrm{C}_f}\left(\left(i^p_{f\alpha} - i^p_{o\alpha}\right) i^p_{f\alpha} + \left(i^p_{f\beta} - i^p_{o\beta}\right) i^p_{f\beta}\right)$$

$$G_Q = \frac{3}{2\mathrm{C}_f}\left(\left(i^p_{f\beta} - i^p_{o\beta}\right) i^p_{f\alpha} - \left(i^p_{f\alpha} - i^p_{o\alpha}\right) i^p_{f\beta}\right)$$

$$H_P = -\frac{3}{2\mathrm{L}_f}\left(\left(v^p_{f\alpha} + R_f i^p_{f\alpha}\right) v^p_{f\alpha} + \left(v^p_{f\beta} + R_f i^p_{f\beta}\right) v^p_{f\beta}\right)$$

$$H_Q = -\frac{3}{2\mathrm{L}_f}\left(\left(v^p_{f\alpha} + R_f i^p_{f\alpha}\right) v^p_{f\beta} - \left(v^p_{f\beta} + R_f i^p_{f\beta}\right) v^p_{f\alpha}\right) \qquad (18)$$

By considering (13), the SM control effort $[\ v^p_{i\alpha} \quad v^p_{i\beta}\ ]^T$ can be obtained by solving the following equation:

$$\frac{\mathrm{d}}{\mathrm{dt}}\begin{bmatrix} S_P \\ S_Q \end{bmatrix} = 0 \qquad (19)$$

By combining (17) and (19), the control law can be obtained as:

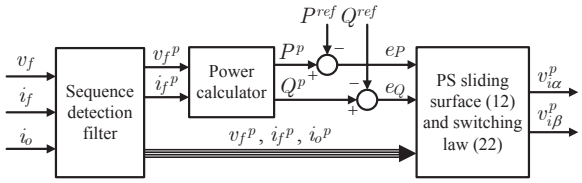

Fig. 3. Proposed control structure for PS power regulation

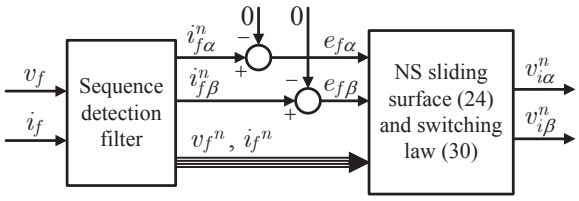

Fig. 4. Structure of NS current controller

$$\begin{bmatrix} v^p_{i\alpha} \\ v^p_{i\beta} \end{bmatrix} = \frac{2\mathrm{L}_f}{3} \begin{bmatrix} v^p_{f\alpha} & v^p_{f\beta} \\ v^p_{f\beta} & -v^p_{f\alpha} \end{bmatrix}^{-1} \left\{ -\begin{bmatrix} G_P \\ G_Q \end{bmatrix} - \begin{bmatrix} H_P \\ H_Q \end{bmatrix} + k_s \begin{bmatrix} e_P \\ e_Q \end{bmatrix} \right\} \tag{20}$$

with:

$$\begin{aligned} \begin{bmatrix} v^p_{f\alpha} & v^p_{f\beta} \\ v^p_{f\beta} & -v^p_{f\alpha} \end{bmatrix}^{-1} &= \frac{-1}{(v^p_{f\alpha})^2 + (v^p_{f\beta})^2} \begin{bmatrix} -v^p_{f\alpha} & -v^p_{f\beta} \\ -v^p_{f\beta} & v^p_{f\alpha} \end{bmatrix} \\ &= \frac{1}{(V^p_f)^2} \begin{bmatrix} v^p_{f\alpha} & v^p_{f\beta} \\ v^p_{f\beta} & -v^p_{f\alpha} \end{bmatrix} \end{aligned} \tag{21}$$

According to SM control theory, the process of SM control can be divided into two phases, that is, the reaching phase and the sliding phase [22]. The control law given by (20) is only valid for sliding phase of the SM control process. The control effort which guarantees the SM control in both the reaching and sliding phases can be represented by [22]:

$$\begin{bmatrix} v^p_{i\alpha} \\ v^p_{i\beta} \end{bmatrix} = \frac{2\mathrm{L}_f}{3(V^p_f)^2} \begin{bmatrix} v^p_{f\alpha} & v^p_{f\beta} \\ v^p_{f\beta} & -v^p_{f\alpha} \end{bmatrix} \left\{ -\begin{bmatrix} G_P \\ G_Q \end{bmatrix} - \begin{bmatrix} H_P \\ H_Q \end{bmatrix} + k_s \begin{bmatrix} e_P \\ e_Q \end{bmatrix} + k_v \begin{bmatrix} \mathrm{sgn}(S_P) \\ \mathrm{sgn}(S_Q) \end{bmatrix} \right\} \tag{22}$$

where$k_v = \mathrm{diag}[k_{vP}, k_{vQ}]$is a diagonal matrix with all positive constant diagonal entries which are the SM control gains and, the sign function$\mathrm{sgn}(\cdot)$is described by:

$$sgn(x) = |x|/x \tag{23}$$

Based on Lyapunov's direct method of stability [22], the overall stability of the control system has been shown in the paper Appendix A. Fig. 3 shows the proposed PS power control scheme.

3.2 Negative-sequence voltage/current control

In order to obtain sinusoidal and symmetrical DG current under unbalanced condition, the NS components of DG current should be eliminated. This can be achieved by introducing the following integral-based sliding surface:

$$\begin{bmatrix} S_{f\alpha} \\ S_{f\beta} \end{bmatrix} = \begin{bmatrix} e_{f\alpha} \\ e_{f\beta} \end{bmatrix} + k_{sf} \int_0^t \begin{bmatrix} e_{f\alpha} \\ e_{f\beta} \end{bmatrix} d\tau \tag{24}$$

where $e_{f\alpha}$ and $e_{f\alpha}$ are the errors between reference and actual values of the NS components of DG current:

$$\begin{cases} e_{f\alpha} = i^{n,ref}_{f\alpha} - i^n_{f\alpha} = -i^n_{f\alpha} \\ e_{f\beta} = i^{n,ref}_{f\beta} - i^n_{f\beta} = -i^n_{f\beta} \end{cases} \tag{25}$$

and $k_{sf} = \mathrm{diag}[k_{sf\alpha}, k_{sf\beta}]$ is a positive constant diagonal matrix. Differentiating (24) with respect to time gives:

$$\begin{aligned} \frac{\mathrm{d}}{\mathrm{dt}} \begin{bmatrix} S_{f\alpha} \\ S_{f\beta} \end{bmatrix} &= \frac{\mathrm{d}}{\mathrm{dt}} \begin{bmatrix} i^{n,ref}_{f\alpha} - i^n_{f\alpha} \\ i^{n,ref}_{f\beta} - i^n_{f\beta} \end{bmatrix} + k_{sf} \begin{bmatrix} e_{f\alpha} \\ e_{f\beta} \end{bmatrix} \\ &= -\frac{\mathrm{d}}{\mathrm{dt}} \begin{bmatrix} i^n_{f\alpha} \\ i^n_{f\beta} \end{bmatrix} + k_{sf} \begin{bmatrix} e_{f\alpha} \\ e_{f\beta} \end{bmatrix} \end{aligned} \tag{26}$$

Substituting for $\frac{\mathrm{d}}{\mathrm{dt}} i^n_{f\alpha\beta}$ from (1) into (26), gives:

$$\begin{aligned} \frac{\mathrm{d}}{\mathrm{dt}} \begin{bmatrix} S_{f\alpha} \\ S_{f\beta} \end{bmatrix} = \frac{R_f}{L_f} \begin{bmatrix} i^n_{f\alpha} \\ i^n_{f\beta} \end{bmatrix} - \frac{1}{L_f} \begin{bmatrix} v^n_{i\alpha} \\ v^n_{i\beta} \end{bmatrix} \\ + \frac{1}{L_f} \begin{bmatrix} v^n_{f\alpha} \\ v^n_{f\beta} \end{bmatrix} + k_{sf} \begin{bmatrix} e_{f\alpha} \\ e_{f\beta} \end{bmatrix} \end{aligned} \tag{27}$$

By considering (13), the SM control effort $[\ v^n_{i\alpha} \quad v^n_{i\beta}\ ]^T$ can be obtained by solving the following equation:

$$\frac{\mathrm{d}}{\mathrm{dt}} \begin{bmatrix} S_{f\alpha} \\ S_{f\beta} \end{bmatrix} = 0 \tag{28}$$

By Combining (27) and (28), it can be obtained that:

$$\begin{bmatrix} v^n_{i\alpha} \\ v^n_{i\beta} \end{bmatrix} = R_f \begin{bmatrix} i^n_{f\alpha} \\ i^n_{f\beta} \end{bmatrix} + \begin{bmatrix} v^n_{f\alpha} \\ v^n_{f\beta} \end{bmatrix} + \frac{1}{L_f} \left\{ k_{sf} \begin{bmatrix} e_{f\alpha} \\ e_{f\beta} \end{bmatrix} \right\} \tag{29}$$

The control law described by (29) is only valid for sliding phase of the SM control process. The control effort

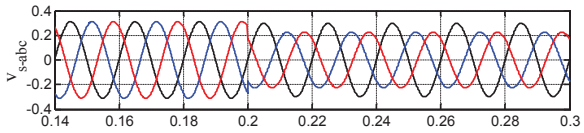

Fig. 5. Grid voltage, during unbalanced condition

which guarantees the SM control in both the reaching and sliding phases can be represented by:

$$\begin{bmatrix} v^n_{i\alpha} \\ v^n_{i\beta} \end{bmatrix} = R_f \begin{bmatrix} i^n_{f\alpha} \\ i^n_{f\beta} \end{bmatrix} + \begin{bmatrix} v^n_{f\alpha} \\ v^n_{f\beta} \end{bmatrix} + \frac{1}{L_f} \left\{ k_{sf} \begin{bmatrix} e_{f\alpha} \\ e_{f\beta} \end{bmatrix} + k_{vf} \begin{bmatrix} \mathrm{sat}(S_{f\alpha}) \\ \mathrm{sat}(S_{f\beta}) \end{bmatrix} \right\} \quad (30)$$

where $k_{vf} = \mathrm{diag}[k_{vf\alpha}, k_{vf\beta}]$ is a positive constant diagonal matrix. The overall stability of the control system has been shown in the paper Appendix B. Based on above equations the proposed NS current control scheme is shown in Fig. 4. In order to avoid unexpected chattering near the sliding surface, the sign function in (22) and (30) is changed into a saturation function, which is described by:

$$\mathrm{sat}(x) = \begin{cases} sgn(x) & |x| > \lambda \\ \mathrm{x}/\lambda & |\mathrm{x}| \leq \lambda \end{cases} \quad (31)$$

where λ is a positive constant. As shown in Fig. 2, only local signals (i_f, v_f and i_o) are used as feedback to control the converters. As depicted in this figure, the positive- and negative-sequence components of the control signals, generated by PS power controller and NS current controller, respectively, are finally summed up to generate the converter voltage references, as an input to space vector modulation (SVM) module.

4 SIMULATION RESULTS

To evaluate the effectiveness of the presented control strategy, the DG study system shown in Fig. 1 has been simulated in the MATLAB/Simulink software environment. The power reference values are given in Table 2, and as stated in section 3.2, the NS current references are zero. The SM control gains are also given in Table 2. In the following graphs, the real powers, reactive powers, voltages and currents are expressed in kilowatts, kilovolt-amperes-reactive, kilovolts and amperes, respectively.

Fig. 5 shows the grid voltage v_{s-abc}, prior and subsequent to an unbalanced voltage disturbance, which can be initiated by heavily unbalanced loading or unsymmetrical fault conditions at the grid side. The unbalanced voltage conditions start at $\mathrm{t} = 0.2$ s with voltage drop of 30%. It

Table 2. Load and Control Parameters

Power references values		
P_{ref}	10 KW	
Q_{ref}	0 VAr	
Loads parameters		
Connected to	R_{load}	L_{load}
PC	25 Ω	60 mH
PCC	10 Ω	24 mH
Control parameters		
$k_{sP},\ k_{sQ}$	1084	
$k_{vP},\ k_{vQ}$	66640	
$k_{sf\alpha},\ k_{sf\beta}$	6×10^4	
$k_{vf\alpha},\ k_{vf\beta}$	6×10^4	
λ	100	

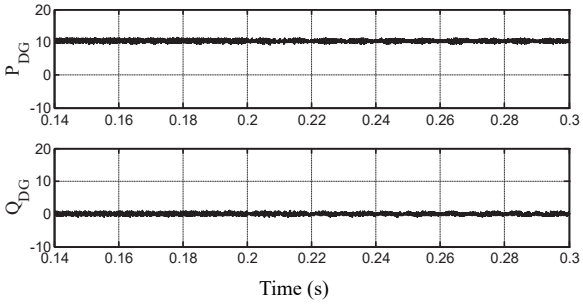

Fig. 6. Instantaneous active and reactive powers, with instantaneous power control method

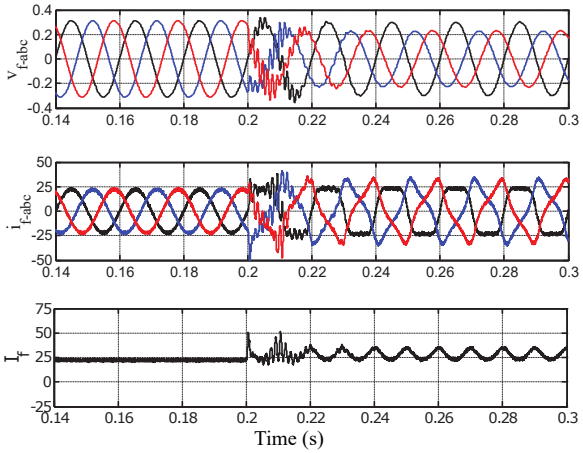

Fig. 7. Waveforms of (a) V_{f-abc}, (b) i_{f-abc} and (c) I_f, with instan-taneous power control method

is assumed that the grid is strong since, the DG unit is not able to assist the grid with its voltage and/or frequency regulation.

For comparison, the described power control method without negative-sequence current compensation is also implemented to regulate the instantaneous active and reac-

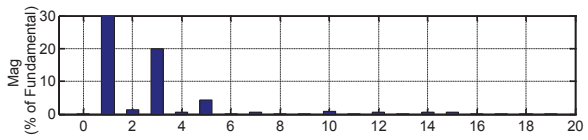

Fig. 8. FFT of the DG phase-b current, with instantaneous power control method

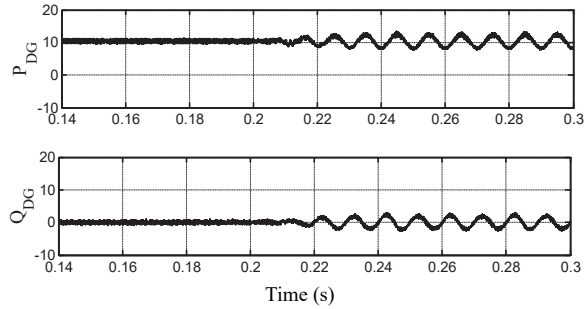

Fig. 9. Instantaneous active and reactive powers, with proposed control method

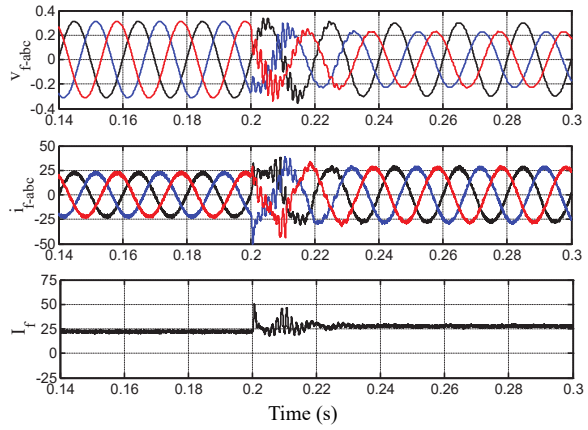

Fig. 10. Waveforms of (a) V_{f-abc}, (b) i_{f-abc} and (c) I_f, with pro-posed control method

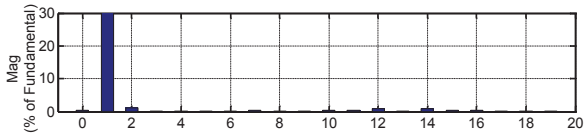

Fig. 11. FFT of the DG phase-b current, with proposed control method

tive powers. The instantaneous active and reactive power components generated by DG unit are shown in Fig. 6. It can be observed that the instantaneous powers track their corresponding reference values under both balanced and unbalanced conditions.

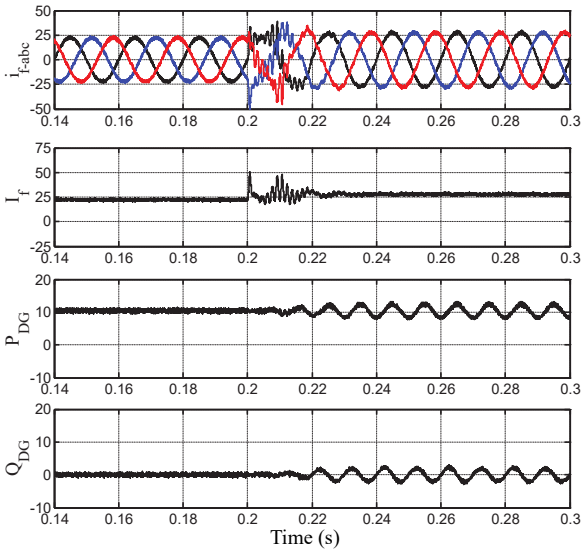

Fig. 12. Waveforms of (a) i_{f-abc}, (b) I_f, (c)P_{DG} and (d) Q_{DG}, with proposed control method, under system parametric un-certainties

Fig. 7 illustrates the waveforms of v_{f-abc}, i_{f-abc} and I_f, over a period around $\mathrm{t} = 0.2$ s, subsequent to the unbalanced voltage disturbance. As shown in Fig. 7(a), due to small size of DG unit, the unbalanced grid voltage can cause the system voltages suffering from high values of negative-sequence which can lead to system voltage imbalance. Therefore, the first term of (11) cannot be directly removed under unbalanced voltage conditions. However, as depicted in Fig. 6, no steady-state double frequency oscillations (DFOs) are observed in the active and reactive powers during the unbalanced conditions. This is due to the fact that the first term and the second term of equation (11) can compensate each other, with instantaneous power control method. Although this method has an acceptable performance in control of instantaneous power under both the balanced and unbalanced conditions, the main limitation of this method is high current distortion during unbalanced conditions, as shown in Fig. 7(b). Fig. 7(c) shows the amplitude of DG output current. This quantity is calculated by:

$$\mathrm{I} = \sqrt{(i_\alpha)^2 + (i_\beta)^2} \tag{32}$$

As indicated, the NS component of the DG output current manifests itself as a DFO in the detected current amplitude. The high-frequency current ripple appeared in Fig. 7(b) is due to the SVM-inverter switching. The fast Fourier transformation (FFT) of phase-b current of DG unit is presented in Fig. 8. The measured total harmonic distortion (THD) of DG output currents is 20.7%.

The results illustrating performance of proposed controller, containing a PS power regulation module and a NS current compensation module, are shown in Figs. 9-11. As shown in Fig. 9, the average value of the active and reactive power of DG unit tracks their respective reference values under both balanced and unbalanced conditions. However, under unbalanced voltage conditions, the instantaneous active and reactive power of DG unit is imposed by DFOs.

Fig. 10 shows the waveforms of v_{f-abc}, i_{f-abc} and I_f, prior and subsequent to the unbalanced voltage disturbance at $\mathrm{t} = 0.2$ s. Fig. 10(b) shows that with proposed control method, the NS components of DG current is very well removed and the DG current reaches its sinusoidal and symmetrical steady-state with a reasonable transient performance. Since the reference value of PS powers of DG unit is constant, the current amplitude increment seen in the waveforms of i_{f-abc}, after $\mathrm{t} = 0.2$ s, is due to amplitude decrement of PS system voltage, under unbalanced voltage conditions.

Although the NS components of DG current are eliminated under unbalanced conditions, due to interaction of PS components of DG current and NS components of DG voltage, the first term of (11) cannot be eliminated and hence, the instantaneous active and reactive power is imposed by DFOs, as shown in Fig. 9. One may note that the amplitude of DFOs is proportional to amplitude of NS components of the system voltage.

The THD value of DG output currents is investigated by analyzing the FFT of phase-b current, as can be seen in Fig. 11. As expected, the measured THD of currents is decreased to 3.5%.

To evaluate the robust performance of proposed controller subject to parametric uncertainties, a 15% step-mismatch is assumed for filter resistance from $\mathrm{t} = 0.18$ s. Some simulation results obtained for this test are shown in Fig. 12. Inspecting these plots, it can be confirmed that the control scheme proposed in this paper is robust and stable with subject to system parameters uncertainties.

5 CONCLUSION

This paper presents a SM based controller for a grid-connected DG unit under unbalanced voltage conditions. The proposed control structure has two control modules consisting of a PS power controller and a NS current controller. The power controller ensures that the PS active and reactive power, generated by DG unit, tracks its respective reference commands under both balanced and unbalanced conditions. The current controller compensates the NS current components of DG unit. The effectiveness of the proposed control structure is demonstrated through time-domain simulation studies, under the MATLAB/Simulink environment. Simulation results confirm that with proposed control method, the NS current components of DG units are removed and, the THD value of the DG output currents are significantly reduced. Simulation results conclude that the proposed control strategy has a reasonable transient response and, is robust and stable subject to system parameters uncertainties.

APPENDIX A

Consider the following positive definite Lyapunov function:

$$V_1 = \frac{1}{2}\begin{bmatrix} S_P & S_Q \end{bmatrix}\begin{bmatrix} S_P \\ S_Q \end{bmatrix} \tag{33}$$

Differentiating V_1 with respect to time gives:

$$\frac{\mathrm{d}}{\mathrm{dt}}V_1 = \begin{bmatrix} S_P & S_Q \end{bmatrix}\left(\frac{\mathrm{d}}{\mathrm{dt}}\begin{bmatrix} S_P \\ S_Q \end{bmatrix}\right) \tag{34}$$

Substituting (17) into (34) yields:

$$\frac{\mathrm{d}}{\mathrm{dt}}V_1 = \begin{bmatrix} S_P & S_Q \end{bmatrix} \left(-\begin{bmatrix} G_P \\ G_Q \end{bmatrix} - \begin{bmatrix} H_P \\ H_Q \end{bmatrix} - \frac{3}{2\mathrm{L}_f}\begin{bmatrix} v^p_{f\alpha} & v^p_{f\beta} \\ v^p_{f\beta} & -v^p_{f\alpha} \end{bmatrix}\begin{bmatrix} v^p_{i\alpha} \\ v^p_{i\beta} \end{bmatrix} + k_s\begin{bmatrix} e_P \\ e_Q \end{bmatrix}\right) \tag{35}$$

By substituting (22) into (35), it can be obtained that:

$$\frac{\mathrm{d}}{\mathrm{dt}}V_1 = \begin{bmatrix} S_P & S_Q \end{bmatrix}\left(-k_v\begin{bmatrix} \mathrm{sgn}(S_P) \\ \mathrm{sgn}(S_Q) \end{bmatrix}\right) \tag{36}$$

The time-derivative of Lyapunov function $\frac{\mathrm{d}}{\mathrm{dt}}V_1$ is then definitely negative so that the power control system becomes asymptotically stable.

APPENDIX B

Choose the following positive definite Lyapunov function:

$$V_2 = \frac{1}{2}\begin{bmatrix} S_{f\alpha} & S_{f\beta} \end{bmatrix}\begin{bmatrix} S_{f\alpha} \\ S_{f\beta} \end{bmatrix} \tag{37}$$

Differentiating V_2 with respect to time gives:

$$\frac{\mathrm{d}}{\mathrm{dt}}V_2 = \begin{bmatrix} S_{f\alpha} & S_{f\beta} \end{bmatrix}\left(\frac{\mathrm{d}}{\mathrm{dt}}\begin{bmatrix} S_{f\alpha} \\ S_{f\beta} \end{bmatrix}\right) \tag{38}$$

Substituting (27) into (38) yields:

$$\frac{\mathrm{d}}{\mathrm{dt}}V_2 = \begin{bmatrix} S_{f\alpha} & S_{f\beta} \end{bmatrix} \left(\frac{R_f}{L_f}\begin{bmatrix} i^n_{f\alpha} \\ i^n_{f\beta} \end{bmatrix} - \frac{1}{L_f}\begin{bmatrix} v^n_{i\alpha} \\ v^n_{i\beta} \end{bmatrix} + \frac{1}{L_f}\begin{bmatrix} v^n_{f\alpha} \\ v^n_{f\beta} \end{bmatrix} + k_{sf}\begin{bmatrix} e_{f\alpha} \\ e_{f\beta} \end{bmatrix}\right) \tag{39}$$

By substituting (30) into (39), it can be obtained that:

$$\frac{\mathrm{d}}{\mathrm{dt}}V_2 = \begin{bmatrix} S_{f\alpha} & S_{f\beta} \end{bmatrix} \left(-k_{vf} \begin{bmatrix} \mathrm{sgn}(S_{f\alpha}) \\ \mathrm{sgn}(S_{f\beta}) \end{bmatrix} \right) \qquad (40)$$

Therefore, the time-derivative of the Lyapunov function $\frac{\mathrm{d}}{\mathrm{dt}}V_2$ is negative definite and the current control system is asymptotically stable.

APPENDIX C

Variables

$\mathbf{v}_i$, $\mathbf{v}_f$, $\mathbf{v}_c$	Inverter, filter, PCC voltage vectors.
$\mathbf{i}_f$, $\mathbf{i}_L$, $\mathbf{i}_l$	Filter, local load, line current vectors.
$v_{\alpha\beta}$, $i_{\alpha\beta}$	$\alpha\beta$ components of voltage and current.
R, L, C	Resistance, inductance, capacitance.
P, Q	Active and reactive powers.
S	Sliding surface
e	Tracking error
ω_s	Synchronous angular frequency.

Superscripts

p, n	Positive-, negative-sequence components.
2ω	Double-frequency oscillating component.
ref	Reference value.

REFERENCES

[1] M. Shahidehpour and F. Schwartz, "Don't let the sun go down on PV," IEEE Power & Energy Magazine, vol. 2, no. 3, pp. 40-48, 2004.

[2] "Special issue on distributed power generation," IEEE Trans. Power Electron., vol. 19, no. 5, Sep. 2004.

[3] Y. A. R. I Mohamed, E. F. El-Saadany, and M. M. A. Salama, "Adaptive grid-voltage sensorless control scheme for inverter-based distributed generation," IEEE Trans. Energy Conv., vol. 24, no. 3, pp. 683-694, Sep. 2009.

[4] M. H. Zahraee, A. Bakhshai, "Transient Droop Control Strategy for Parallel Operation of Voltage Source Converters in an Islanded Mode Microgrid", 33rd International Telecommunications Energy Conference (INTELEC), IEEE, 9-13 Oct. 2011.

[5] N. Pogaku, M. Prodanovic, and T. Green, "Modeling, analysis and testing of autonomous operation of an inverter-based microgrid," IEEE Trans. Power Electron., vol. 22, no. 2, pp. 613–625, Mar. 2007.

[6] Y. Li and Y.W. Li, "Power management of inverter interfaced autonomous microgrid based on virtual frequency-voltage frame," IEEE Trans. Smart Grid, vol. 2, no. 1, pp. 30–40, Mar. 2011.

[7] F. Katiraei and M. R. Iravani, "Power management strategies for a microgrid with multiple distributed generation units," IEEE Trans. Power Syst., vol. 21, pp. 1821–1831, Nov. 2006.

[8] G. Saccomando and J. Svensson, "Transient operation of grid-connected voltage source converter under unbalanced voltage conditions," in *Proc. Ind. Appl. Conf., 36th IAS Annu. Meeting*, 2001, vol. 4, pp. 2419–2424.

[9] M. Castilla, J. Miret, J. L. Sosa, J. Matas, and L. G. de Vicuna, "Grid-fault control scheme for three-phase photovoltaic inverters with adjustable power quality characteristics," IEEE Trans. Power Electron., vol. 25, no. 12, pp. 2930-2940, Dec. 2010.

[10] Z. Guowei, B.China, W. Tongzhen, H. Shengli and K. Lingzhi, "The Control for Grid Connected Inverter of Distributed Generation under Unbalanced Grid Voltage," in *proc. International Conference on Sustainable Power Generation and Supply, 2009. SUPERGEN '09,* Apr. 2009, pp. 1–5.

[11] M. H. J. Bollen, "Algorithms for characterizing measured three-phase unbalanced voltage dips," IEEE Trans. Power Delivery, vol. 18, no. 3, pp. 937–944, Jul. 2003.

[12] A. Hajizadeh, M. A. Golkar, and A. Feliachi, "Voltage control and active power management of hybrid fuel-cell/energy-storage power conversion system under unbalanced voltage sag conditions," IEEE Trans. Energy Conv., vol. 25, no. 4, pp. 1195-1208 Dec. 2010.

[13] A. Yazdani and R. Iravani, "A Unified Dynamic Model and Control for the Voltage-Sourced Converter Under Unbalanced Grid Conditions," IEEE Trans. Power Delivery, vol. 21, no. 3, pp. 1620-1629, July 2006.

[14] F. Wang, J. L. Duarte, and M. A. M. Hendrix, "Pliant active and reactive power control for grid-interactive converters under unbalanced voltage dips," IEEE Trans. Power Electron., vol. 26, no. 5, pp. 1511–1521, May 2011.

[15] J. A. Suul, A. Luna, P. Rodriguez, and T. Undeland, "Virtual-flux-based voltage-sensor-less power control for unbalanced grid conditions," IEEE Trans. Power Electron., vol. 27, no. 9, Sep. 2012.

[16] L. Shang, D. Sun and J. Hu, "Sliding-mode-based direct power control of grid-connected voltage-sourced inverters under unbalanced network conditions," IET Power Electron., vol. 4, no. 5, pp. 570–579, 2011.

[17] L. Shang and J. Hu, "Sliding-Mode-Based Direct Power Control of Grid-Connected Wind-Turbine-Driven Doubly Fed Induction Generators under Unbalanced Grid Voltage Conditions," IEEE Trans. Energy Conv., vol. 27, no. 2, Jun. 2012.

[18] Y. Zhou, P. Bauer, J. Ferreira and J. Pierik, "Operation of grid-connected DFIG under unbalanced grid voltage condition," IEEE Trans. Energy Conv., vol. 24, no 1, pp. 240–246, March 2009.

[19] F. Wang, J. Duarte and M. Hendrix, "High performance stationary frame filters for symmetrical sequences or harmonics separation under a variety of grid conditions," in *Proc. IEEE APEC*, 2009, pp. 1570–1576.

[20] A. Sallam and O. Malik, "Voltage Variations, in Brown," *Electric Distribution Systems*, New Jersey, USA: Wiley-IEEE, 2011, 1st ed., pp. 319-320.

[21] S. Vazquez, J.A. Sanchez, R. Reyes, J.I. Leon and J.M. Carrasco, "Adaptive Vectorial Filter for Grid Synchronization of Power Converters under Unbalanced and/or Distorted Grid Conditions," IEEE Trans. Ind. Electron., 2014, 61, pp. 1355–1367.

[22] J. E. Slotine and W. Li, *Applied Nonlinear Control*, Englewood Cliffs, NJ: Prentice-Hall, 1991.

Mohammad Mahdi Rezaei received the M.Sc. degree in electrical engineering from Amirkabir University of Technology (Tehran Polytechnic), Tehran, Iran, in 2007, and the Ph.D. degree in electrical engineering from the Science and Research Branch, Islamic Azad University, Tehran, Iran, in 2015. He is currently an Assistant Professor in the Department of Electrical and Computer Engineering, Khomeinishahr Branch, Islamic Azad University, Isfahan, Iran. His main areas of research are control of microgrids, distributed generations, and design, optimization and implementation of electrical drives.

Jafar Soltani received the M.Sc. and Ph.D. degrees from the University of Manchester Institute of Science and Technology (UMIST), Manchester, U.K., in 1983 and 1987, respectively. He is currently a Professor in the Department of Electrical Engineering, Khomeinishar Branch, Islamic Azad University, Isfahan, Iran. He is also an Emeritus Professor with the Faculty of Electrical and Computer Engineering, Isfahan University of Technology, Isfahan, Iran. His main area of research is electrical machines and drive, power electronics, and power system control. He has published many international journal and conference papers and is the holder of a U.K. patent. Dr. Soltani is a member of IEEE. In addition, he is the reviewer of some international journals in European and IEEE Transactions.

AUTHORS' ADDRESSES

M.M. Rezaei, M.Sc.
Department of Electrical and Computer Engineering,,
Khomeinishahr Branch,
Islamic Azad University,
Isfahan, Iran
email: mm.rezaei@iaukhsh.ac.ir

Prof. J. Soltani, Ph.D.
Department of Electrical and Computer Engineering,,
Khomeinishahr Branch,
Islamic Azad University,
Isfahan, Iran
email: jsoltani@iaukhsh.ac.ir

Received: 2014-05-17
Accepted: 2015-03-17